EPJ Web of Conferences **271**, 08004 (2022) https://doi.org/10.1051/epjconf/202227108004
HYP2022

New results on light nuclei, hyperons and hypernuclei from HADES

(HADES collaboration)

Rayane Abou Yassine[6,14], *Jörn* Adamczewski-Musch[5], *Marten* Becker[10], *Philip* Bergmann[5], *Alberto* Blanco[1], *Christoph* Blume[8], *Lukas* Chlad[15,21], *Petr* Chudoba[15], *Izabela* Ciepał[3], *Malte* Cordts[6], *Jörn* Dreyer[7], *Waleed Ahmed* Esmail[5], *Miroslaw* Firlej[2], *Tomasz* Fiutowski[2], *Henrik* Floersheimer[6], *Paulo* Fonte[1,19], *Jürgen* Friese[9], *Ingo* Fröhlich[8], *Jörg* Förtsch[18], *Tetyana* Galatyuk[6,5], *Tomasz* Gniazdowski[17], *Robert* Greifenhagen[7,20], *Mateusz* Grunwald[17], *Dieter* Grzonka[11], *Malgorzata* Gumberidze[5], *Szymon* Harabasz[6], *Thorsten* Heinz[5], *Claudia* Höhne[10,5], *Fatima* Hojeij[14], *Romain* Holzmann[5], *Holger* Huck[8], *Marek* Idzik[2], *Burkhard* Kämpfer[7,20], *Karl-Heinz* Kampert[18], *Behruz* Kardan[8], *Vadym* Kedych[6], *Ilse* Koenig[5], *Wolfgang* Koenig[5], *Marvin* Kohls[8], *Jedrzej* Kolas[17], *Grzegorz* Korcyl[4], *Georgy* Kornakov[17], *Frederic* Kornas[6,5], *Roland* Kotte[7], *Wilhelm* Krueger[6], *Andrej* Kugler[15], *Pawel* Kulessa[11], *Rafal* Lalik[4], *Semen* Lebedev[10], *Sergey* Linev[5], *Luís* Lopes[1], *Manuel* Lorenz[8], *Akshay* Malige[4], *Jochen* Markert[5], *Tomasz* Matulewicz[16], *Johan* Messchendorp[5], *Volker* Metag[10], *Jan* Michel[8], *Aleksandra* Molenda[2], *Jakub* Moron[2], *Christian* Müntz[8], *Marvin* Nabroth[8], *Lothar* Naumann[7], *Jan* Orliński[16], *Jan-Hendrik* Otto[10], *Yannis* Parpottas[12], *Mirco* Parschau[8], *Christian* Pauly[18], *Vladimir* Pechenov[5], *Olga* Pechenova[5], *Gabriela* Perez Andrade[11], *Dennis* Pfeifer[18], *Krzysztof* Piasecki[16], *Jerzy* Pietraszko[5], *Tetiana* Povar[18], *Alexandr* Prozorov[15,21], *Witold* Przygoda[4], *Krzysztof* Pysz[3], *Béatrice* Ramstein[14], *Narendra* Rathod[4], *James* Ritman[5], *Adrian* Rost[6,5], *Anar* Rustamov[5], *Piotr* Salabura[4], *Joao* Saraiva[1], *Susan* Schadmand[5], *Niklas* Schild[6], *Erwin* Schwab[5], *Florian* Seck[6], *Ilya* Selyuzhenkov[5], *Udai* Singh[4], *Leon* Skorpil[8], *Jerzy* Smyrski[4], *Manfred* Sobiella[7], *Stefano* Spataro[22], *Simon* Spies[8,*], *Maria* Stefaniak[17], *Herbert* Ströbele[8], *Joachim* Stroth[8,5], *Konrad* Sumara[4], *Ondřej* Svoboda[15], *Krzysztof* Swientek[2], *Melanie* Szala[8], *Pavel* Tlusty[15], *Michael* Traxler[5], *Haralabos* Tsertos[12,13], *Vladimir* Wagner[15], *Mateusz* Wasiluk[17], *Adrian Amatus* Weber[10], *Christian* Wendisch[5], *Peter* Wintz[11], *Hanna* Zbroszczyk[17], *Elizaveta* Zherebtsova[5,23], *Marcin* Zielinski[4], and *Peter* Zumbruch[5]

[1]LIP-Laboratório de Instrumentação e Física Experimental de Partículas , 3004-516 Coimbra, Portugal
[2]AGH University of Science and Technology, Faculty of Physics and Applied Computer Science, 30-059 Kraków, Poland
[3]Institute of Nuclear Physics, Polish Academy of Sciences, 31342 Kraków, Poland
[4]Smoluchowski Institute of Physics, Jagiellonian University of Cracow, 30-059 Kraków, Poland
[5]GSI Helmholtzzentrum für Schwerionenforschung GmbH, 64291 Darmstadt, Germany
[6]Technische Universität Darmstadt, 64289 Darmstadt, Germany
[7]Institut für Strahlenphysik, Helmholtz-Zentrum Dresden-Rossendorf, 01314 Dresden, Germany
[8]Institut für Kernphysik, Goethe-Universität, 60438 Frankfurt, Germany
[9]Physik Department E62, Technische Universität München, 85748 Garching, Germany
[10]II.Physikalisches Institut, Justus Liebig Universität Giessen, 35392 Giessen, Germany
[11]Forschungszentrum Juelich, 52428 Juelich, Germany

[*]e-mail: s.spies@gsi.de

[12]Frederick University, 1036 Nicosia, Cyprus
[13]Department of Physics, University of Cyprus, 1678 Nicosia, Cyprus
[14]Laboratoire de Physique des 2 infinis Irène Joliot-Curie, Université Paris-Saclay, CNRS-IN2P3. , F-91405 Orsay , France
[15]Nuclear Physics Institute, The Czech Academy of Sciences, 25068 Rez, Czech Republic
[16]Uniwersytet Warszawski - Instytut Fizyki Doświadczalnej, 02-093 Warszawa, Poland
[17]Warsaw University of Technology, 00-662 Warsaw, Poland
[18]Bergische Universität Wuppertal, 42119 Wuppertal, Germany
[19]also at Coimbra Polytechnic - ISEC, Coimbra, Portugal
[20]also at Technische Universität Dresden, 01062 Dresden, Germany
[21]also at Charles University, Faculty of Mathematics and Physics, 12116 Prague, Czech Republic
[22]also at Dipartimento di Fisica and INFN, Università di Torino, 10125 Torino, Italy
[23]also at University of Wrocław, 50-204 Wrocław, Poland

Abstract. In March 2019 the HADES experiment recorded 14 billion Ag+Ag collisions at $\sqrt{s_{NN}} = 2.55$ GeV as a part of the FAIR phase-0 physics program. In this contribution, we present and investigate our capabilities to reconstruct and analyze weakly decaying strange hadrons and hypernuclei emerging from these collisions. The focus is put on measuring the mean lifetimes of these particles.

1 Introduction

In heavy-ion collisions in the energy regime of few GeV per nucleon, which are explored by HADES, the nuclear matter is heated to temperatures of 70 MeV deduced from dielectron spectroscopy [1]. At the same time, it is compressed to densities above its ground state density. Densities and temperatures of the same order of magnitude are also expected in merging neutron stars [2, 3]. For this reason, the study of these few GeV heavy-ion collisions allows us to gain information on the microscopic composition and also deduce macroscopic properties like the equation of state of astronomic objects like merging neutron stars.

1.1 Strange hadron and hypernuclei production

At collision energies of few GeV, the lightest strange mesons, the Kaons, as well as the lightest hyperons, the Λ hyperons, are produced close to their free nucleon nucleon threshold energy. Therefore, their excitation function experiences a steep rise with increasing $\sqrt{s_{NN}}$, while the production rates are at the order of $\lesssim 0.1$ per collision [4–6]. At the same time, nucleons from the colliding nuclei are stopped noticeably in the collision zone and dominate the fireball. This offers excellent conditions for the formation and emission of light nuclei as well as hypernuclei involving one (or more) hyperons [7]. Hypernuclei allow us to probe the underlying hyperon-nucleon interactions which are highly relevant for the equation of state at high densities [8, 9]. Furthermore, the production rates and kinematic distributions of hypernuclei are investigated to determine their dominant formation mechanism (e.g. thermal production, coalescence [10]).

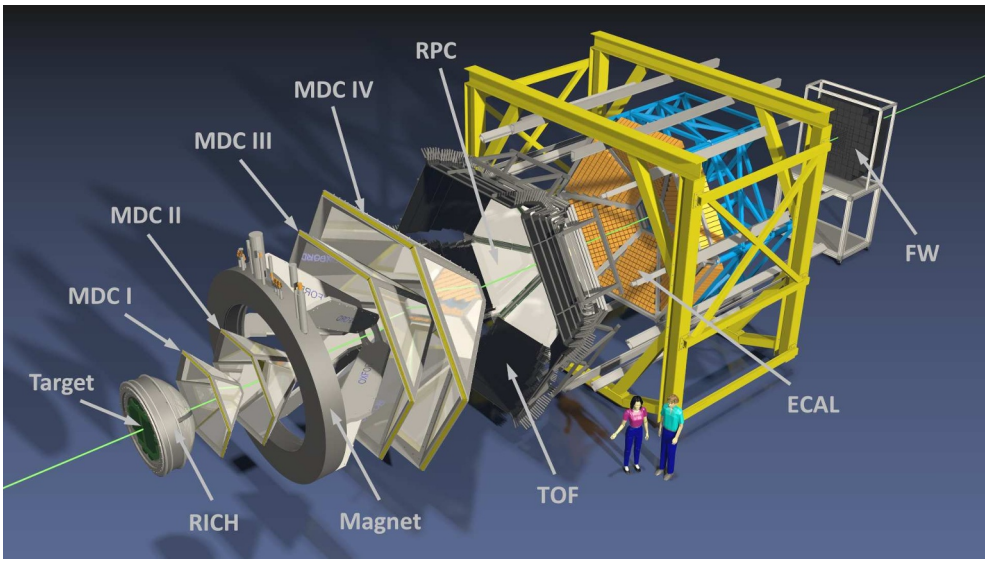

Figure 1. Schematic expanded view of the HADES detector setup.

2 HADES experiment

The HADES experiment, which is schematically depicted in an expanded view in Fig. 1, is a multi-purpose high-acceptance compact magnet spectrometer. It is operated in a fixed-target mode using beams from the SIS18 accelerator at GSI, Darmstadt, Germany. Besides heavy-ion A+A collisions, also elementary p+A and p+p as well as pion induced π+A collisions are measured, e.g. [11–13]. Starting from the segmented 15-fold silver target, the particles traverse a Ring-Imaging CHerenkov (RICH) detector for e^+/e^- identification, two low-mass Mini Drift Chamber (MDC) tracking stations, a toroidal magnetic field, followed by two further MDC tracking stations and depending on the polar angle either a Resistive Plate Chamber (RPC) or a Time of Flight (ToF) scintillation detector for a time of flight measurement. The setup is completed by an Electromagnetic CALorimeter (ECAL) for photon detection, a Forward Wall (FW) hodoscope for measurement of the event plane and a diamond reaction time and trigger detector (START) located in front of the target. Besides the RICH, the FW and the START detector, all detectors are split into six independent sectors covering almost the entire azimuthal angle. More details on the HADES experiment are given in [14].

3 Weak decay recognition

While the charged kaons have a mean flight length $c\tau$ of a few meters and are thereby measured directly in the detectors, the Λ hyperon, K^0_S meson and all known hypernuclei have mean flight lengths $c\tau$ of only a few centimeters and thereby need to be reconstructed from their decay daughters. The large amount of protons, pions and light nuclei, not associated with weak decays, makes a method to effectively separate the signals from the combinatorial background inevitable. For this purpose, the macroscopic mean flight lengths $c\tau$ of weakly decaying particles are utilized, resulting in a spatial displacement between the primary event vertex and the secondary decay vertex which can be detected. This displacement further leads to a so-called *Off-Vertex-Decay-Topology* which is quantified using the following parameters defined in the laboratory reference system:

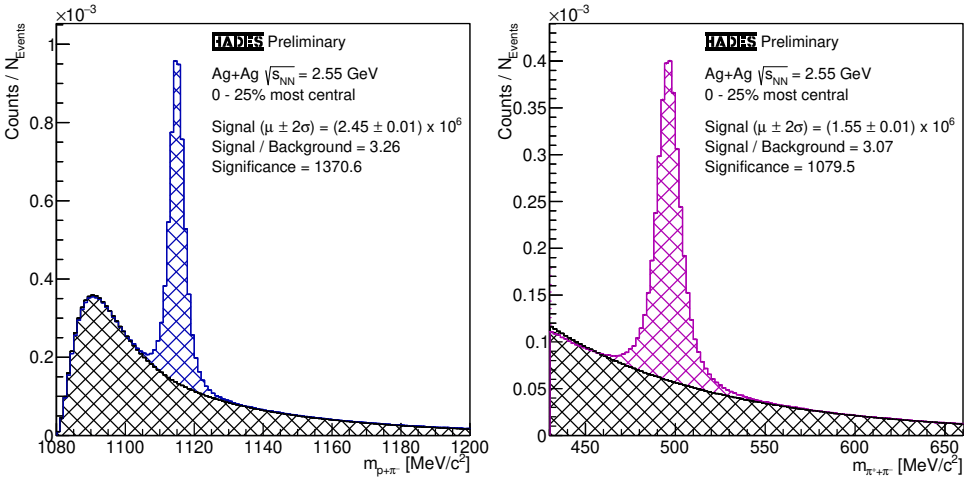

Figure 2. Invariant mass spectra of $\Lambda \rightarrow p + \pi^-$ decays (left) and $K^0_S \rightarrow \pi^+ + \pi^-$ decays (right) from the 0-25% most central Ag(1.58A GeV)+Ag events measured by HADES.

- Distance between the primary and secondary vertices.
- Distance of closest approach (DCA) between the daughter tracks and the primary vertex.
- DCA between reconstructed mother track and primary vertex.
- DCA between the two daughter tracks.
- Opening angle between the two daugther tracks.

In addition, the method proposed by R. Armenteros and J. Podolanski [15] is used to take the kinematic constraints of two-body decays into account as described in [6, 16]. Finally, the procedure is completed by using a Multi-Layer-Perceptron (MLP) artificial Neural Network (aNN) from the Toolkit for Multivariate Data Analysis (TMVA) [17] to further enhance the rejection of combinatorial background. For this purpose, the Off-Vertex-Decay-Topology parameters except for the opening angle as well as the azimuthal angle of the Armenteros-Podolanski ellipse (cf. [6, 16]) are used as input parameters of the aNN which is trained using simulated signal samples and background samples obtained by the mixed-event technique.

In previous analyses [5, 18] it is demonstrated that the use of an aNN to reject the combinatorial background in the recognition procedure of weak decays significantly improves the statistical significance of the reconstructed signals compared to pure hard-cut analyses. In total, the reconstruction method allows the reconstruction of 2.45 million Λ hyperons and 1.55 million K^0_S mesons in the relevant two-body decay channels as shown in the invariant mass distributions in Fig. 2.

4 Lifetime measurements

To achieve proper measurements of the mean lifetimes of ${}^{3}_{\Lambda}H$ and ${}^{4}_{\Lambda}H$ hypernuclei, first, the method has to be assessed to prevent systematic effects coming from e.g. the required correction factors for acceptance and efficiency effects. Therefore, the mean lifetimes of Λ hyperons and K^0_S mesons are ideally suited, since they are measured with high precision by many experiments and do not depend on the production mechanism of the particle. Besides that, the

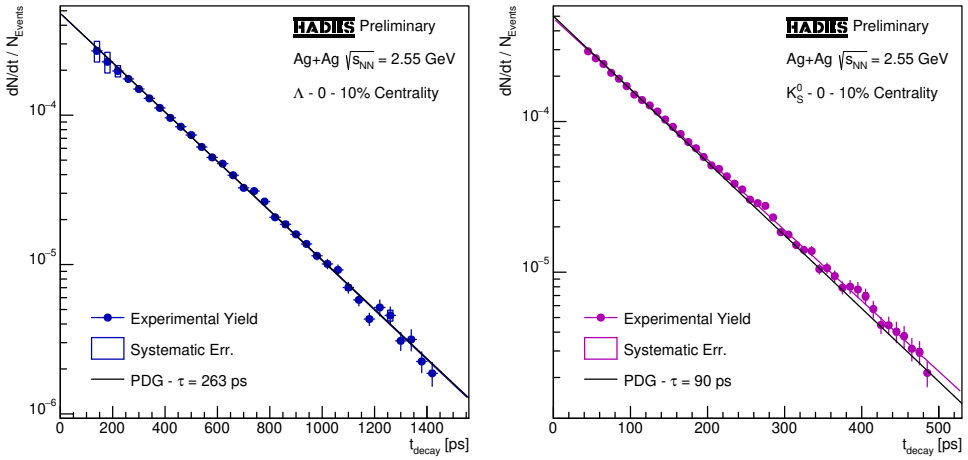

Figure 3. Decay curves of Λ hyperons (left) and K^0_S mesons (right) from the 0-10% most central Ag(1.58A GeV)+Ag events measured by HADES. The colored lines correspond to the exponential fit functions and the black lines to the PDG literature lifetimes [19].

highly significant signals of these particles allow for studies with vanishing statistical uncertainties. In the following, the measurement technique for mean lifetimes of weakly decaying hadrons is described.

The decay time t of a particle is calculated from its decay length l, its velocity β and its Lorentz-factor γ via equation 1:

$$t = \frac{l}{\beta\gamma c} \tag{1}$$

Using the calculated decay times, the reconstructed Λ hyperons are distributed to 37 equally sized intervals of 40 ps width ranging from 120 to 1600 ps, and the reconstructed K^0_S mesons are distributed to 46 equally sized intervals of 10 ps width ranging from 40 to 500 ps. In each interval, the amount of reconstructed particles is extracted from the corresponding invariant mass spectrum in a $\pm 2\sigma$ range determined by Gaussian fit functions.

These extracted signal counts are corrected for acceptance and efficiency losses using simulated Λ hyperons and K^0_S mesons generated according to the kinematic distributions determined in the multi-differential analyses described in [6]. For a given decay time, the kinematic distributions strongly influence the distribution of decay lengths which further influences the integrated acceptance and efficiency correction factors. Thus, proper kinematic distributions are mandatory. The simulated particles are processed by the HGeant package, based on the GEometry And TRacking (GEANT) 3.21 package [20], to emulate their interactions with the detector materials and the corresponding detector responses. Afterward, they are merged with actually measured events and processed by the full event reconstruction procedure to determine their acceptance and efficiency correction factors (cf. [6]).

Using this procedure, the decay curves shown in figure 3 are obtained. They are fitted with an exponential function representing the decay law according to equation 2 to extract the mean lifetime of Λ hyperons and K^0_S mesons:

$$N(t) = N_0 \cdot \exp\left(-\frac{t}{\tau}\right) \Rightarrow \frac{dN}{dt} = -\frac{N_0}{\tau} \cdot \exp\left(-\frac{t}{\tau}\right) \tag{2}$$

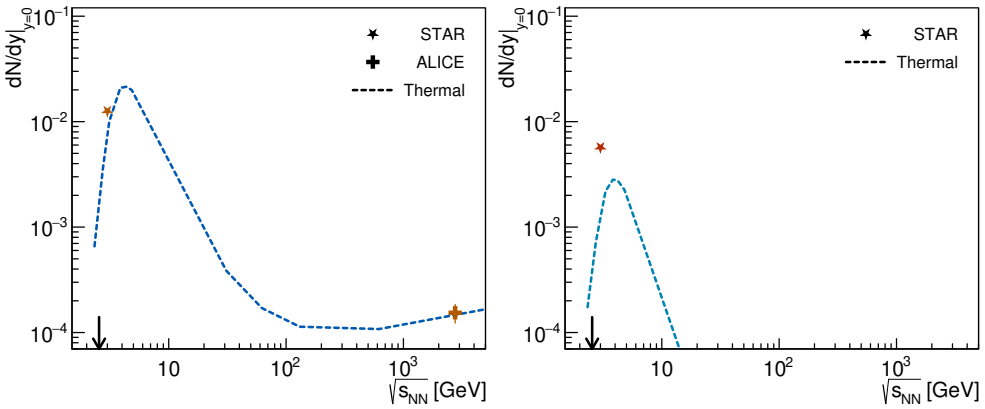

Figure 4. Energy excitation functions of the ${}^{3}_{\Lambda}$H (left) and ${}^{4}_{\Lambda}$H (right) production rates at mid-rapidity. The data are taken from [7, 21]. The dashed lines correspond to thermal model predictions [22] taken from [7] as well.

The obtained mean lifetimes τ of (262 ± 2 ± 3) ps (Λ) and (92 ± 1 ± 1) ps (K^0_S) are both in accordance with the corresponding literature lifetimes of 263 ps and 90 ps [19]. The first given uncertainty is of statistical nature, while the second one is of systematic nature and obtained by altering selection criteria used for the identification of the corresponding decay candidates. These alternative selection criteria correspond to pure hard-cut analyses, which is why any systematic effect that might arise from using the aNN is included in the systematic uncertainties. This proves that the HADES spectrometer as well as the applied procedures are suited to measure the lifetimes of weakly decaying hadrons.

5 Production rates

Fig. 4 shows the energy excitation functions of ${}^{3}_{\Lambda}$H and ${}^{4}_{\Lambda}$H production rates at mid-rapidity. At the moment only very few data on the production of hypernuclei in heavy-ion collisions at mid-rapidity are available. Therefore, the currently available data set leaves space for various different model predictions. Yet, the general trend is clear. At collision energies at or below the energy threshold of hyperon production in binary NN collisions, the production of hypernuclei is limited by the availability of produced hyperons, and their energy excitation function shows an exponential increase. In the energy region $\sqrt{s_{NN}} \gtrsim 10$ GeV, the number of nuclei present in the collision system ceases as discussed in Sec. 1.1. Therefore, the production rates of hypernuclei are decreasing again resulting in a maximum of hypernuclei production in the energy region of $\sqrt{s_{NN}} \approx$ 3-6 GeV. Heavier hypernuclei are stronger affected by the ceasing amount of nucleons in the collision system which is why they develop maximal production rates at lower energies than lighter hypernuclei.

The thermal predictions depicted by the dashed lines in Fig. 4 which are supported by the available data points show these discussed effects. However, deeper and more quantitative investigations of the mechanisms relevant to the formation of Hypernuclei in heavy-ion collisions require further measurements from different energies and collision systems.

6 Summary and outlook

In this contribution, we have presented benchmark measurements of Λ hyperons and K^0_S mesons demonstrating the capability of HADES for high-precision lifetime measurements of weakly decaying particles. In the next step, the lifetimes of the currently accessible hypernuclei, the ${}^{3}_{\Lambda}$H and the ${}^{4}_{\Lambda}$H, are going to be measured which might provide further constraints to models describing the highly relevant hyperon-nucleon interactions.

Furthermore, we discussed the energy excitation function of hypernuclei production and the requirement for more independent measurements to constrain it. In particular, the upcoming CBM experiment, which will operate in the energy region of $\sqrt{s_{NN}} \approx$ 3-6 GeV where maximal hypernuclei production rates are expected, is going to provide very valuable data on hypernuclei. Also, the final results from the most recent STAR fixed-target measurement campaign will significantly extend the available data set on hypernuclei production in heavy-ion collisions.

In parallel to the ongoing analysis of the Ag(1.58A GeV)+Ag data, the HADES collaboration is implementing the Kalman-Filter based KF-Particle-Finder [23] package to reconstruct decaying particles. This approach is already employed by STAR, ALICE and CBM to increase the reconstruction efficiencies of decaying particles. Thereby, it will strongly enhance the reconstruction and analysis of hypernuclei, in particular with respect to three-body decay channels to reconstruct for example the ${}^{4}_{\Lambda}$He.

We gratefully acknowledge the support by SIP JUC Cracow, Cracow (Poland), 2017/26/M/ST2/00600; TU Darmstadt, Darmstadt (Germany), VH-NG-823, DFG GRK 2128, DFG CRC-TR 211, BMBF:05P18RDFC1; Goethe-University, Frankfurt (Germany) and TU Darmstadt, Darmstadt (Germany), DFG GRK 2128, DFG CRC-TR 211, BMBF:05P18RDFC1, HFHF, ELEMENTS:500/10.006, VH-NG-823, GSI F&E, ExtreMe Matter Institute EMMI at GSI Darmstadt; JLU Giessen, Giessen (Germany), BMBF:05P12RGGHM; IJCLab Orsay, Orsay (France), CNRS/IN2P3; NPI CAS, Rez, Rez (Czech Republic), MSMT LTT17003, MSMT LM2018112, MSMT OP VVV CZ.02.1.01/0.0/0.0/18_046/0016066.

References

[1] J. Adamczewski-Musch *et al.* HADES Collaboration, Nature Phys. **15** 1040-1045 (2019).
[2] M. Hanauske, J. Steinheimer, L. Bovard, A. Mukherjee, S. Schramm *et al.*, J. Phys. Conf. Ser. **878** 012031 (2017)
[3] C. Ecker, M. Järvinen, G. Nijs and W. van der Schee, Phys. Rev. D **101** 103006 (2020)
[4] V. Steinberg, J. Staudenmaier, D. Oliinychenko, F. Li, Ö. Erkiner and H. Elfner, Phys. Rev. C **99**, 064908 (2019)
[5] J. Adamczewski-Musch *et al.* HADES Collaboration, Phys. Lett. B **793** 457-463 (2019)
[6] S. Spies, PhD Thesis Goethe Universität Frankfurt (2022)
[7] M. Abdallah *et al.* STAR Collaboration, Phys.Rev.Lett. **128** 20, 202301 (2022)
[8] T. Saito *et al.*, Nature Rev.Phys. **3** 12, 803-813 (2021)
[9] A. Gal, E. V. Hungerford, and D. J. Millener, Rev.Mod.Phys. **88**, 035004 (2016)
[10] J. Steinheimer, K. Gudima, A. Botvina, I. Mishustin, M. Bleicher and H. Stöcker, Phys. Lett. B **714** 85-91 (2012)
[11] G. Agakishiev *et al.* HADES Collaboration, Eur. Phys. J. A **50** 81 (2014)
[12] J. Adamczewski-Musch *et al.* HADES Collaboration, Phys.Rev.C **95** 015207 (2017)
[13] J. Adamczewski-Musch *et al.* HADES Collaboration, Phys. Rev. C **102** 024001 (2020)
[14] G. Agakishiev *et al.* HADES Collaboration, Eur. Phys. J. A **41** 243-277 (2009)
[15] J. Podolanski and R. Armenteros, Phil. Mag. **45** 13-30 (1954)
[16] S. Spies, EPJ Web Conf. **259** 01007 (2022)
[17] A. Hocker, P. Speckmayer, J. Stelzer, J. Therhaag, E. von Toerne *et al.*, TMVA - Toolkit for Multivariate Data Analysis, CERN-OPEN-2007-007 (2007)
[18] S. Spies, J. Phys. Conf. Ser. **1667** 012041 (2020)
[19] R.L. Workman *et al.* Particle Data Group, Prog.Theor.Exp.Phys. **2022**, 083C01 (2022)
[20] R. Brun, F. Bruyant, M. Maire, A.C. McPherson and P. Zanarini, CERN-DD-EE-84-1 (1987)
[21] J. Adam *et al.* ALICE Collaboration, Phys. Lett. B **754** 360-372 (2016)
[22] A. Andronic, P. Braun-Munzinger, J. Stachel and H. Stöcker, Phys. Lett. B **697** 203-207 (2011)
[23] S. Gorbunov and I. Kisel, CBM-SOFT-note-2007-003 (2007)